BNL-62370

Behavior of Dissolved Molybdenum during Localized Corrosion of Austenitic Stainless Steel

H. S. Isaacs and S-M Huang
Department of Applied Science, Brookhaven National Laboratory, Upton NY 11973, USA.

Abstract

An *in situ* study of the chemistry of molybdenum during localized of corrosion of stainless steel in chloride solutions has been carried using energy dispersive x-ray techniques. An artificial pit was used to maintained a one dimensional diffusion geometry by dissolving back the cross section of strip of Type 316 stainless steel foil mounted in an epoxy resin. A high intensity 8 μm diameter polychromatic x-ray beam at Beamline x26A was scanned across the steel, a salt layer on the steel, and the concentrated dissolution products within the artificial pit. The resulting x-ray fluorescence was analyzed to determine changes in concentration of the constituent alloying elements. It has been found that the salt layer on the steel was formed mainly by iron chloride and all other alloying elements were present at relatively lower concentrations than n the steel. Virtually no chromium remained in the salt layer. Also, little molybdenum was present negating proposed corrosion inhibition by a definitive molybdenum forming salt layer. Within the concentrated artificial pit solution it was found that alloying elements dissolved and migrated down a concentration gradient, but closer to the mouth of deep (~2 mm) pits, precipitation of molybdenum occurred to a minor extent that did not affect the localized corrosion processes.

Introduction

Molybdenum leads to marked improvements in the corrosion resistance of stainless steels and differing models of action have been proposed for the reduction of corrosion. Models may be broadly classified according to whether Mo acts in the active or passive state. In the passive state Mo may enter and change the passive oxide film improving its resistance to breakdown (1,2). In the active state, Mo acts to reduce the dissolution rate of the bare metal during localized corrosion, facilitating repassivation of pits. This occurs by absorbing preferentially on the dissolving surface (3) or by enhancing precipitation of a Mo rich salt layer on the active surface (4-6). Reduction of the active dissolution kinetics reduces the rate of chloride replacement lost by diffusion from the pit thereby enabling repassivation that takes place below a critical concentration of dissolved metal chlorides (7).

Recently it has been shown that the composition of salt layers on alloys can be determined using *in situ* x-ray microprobe analysis.(8) The work reported here employs these energy dispersive x-ray (EDX) techniques to determine the distribution of elements in an artificial type 316 stainless steel pit.

Experimental

A schematic of the electrochemical call used for energy dispersive x-ray analysis (EDX) is shown in Fig. 1. Like the wire used in "lead-in-pencil" electrodes the cross section of the foil was dissolved to form a pit or crevice and diffusion from the metal to the mouth of the pit, simulated a one-dimensional geometry. A Type 316 stainless steel foil electrode was sandwiched between plastic sheets . The foil was prepared by cold rolling that produced a rough surface. The required thickness of the foil was determined considering absorption of Cr K fluorescent x-rays in the steel. A thickness of 15 μm was chosen so that the calculated fluorescence yield was still dependent on foil thickness. SEM measurements showed the thickness varied from 10 to 15 μm over distances of about 30 μm. The distances between The composition of the steel was 0.04 C, 0.36 Si, 0.028 P, 0.001S, 16.41 Cr, 1,54 Mn, 10.13 Ni, and 2.10 Mo in weight percent .The potential of the steel foil as it dissolved back during the x-ray measurements was controlled potentiostatically relative to a calomel electrode. The bulk solution contained 1.0 M HCl and 1.0M LiCl.

A 13-element solid state detector, positioned at 90° to the incident polychromatic x-ray beam from the light source, was used for energy discrimination of the fluorescent signal from the sample. The beam diameter was collimated to nominally 8 μm. The cell was mounted on an X-Y-Z stage to control the point of incidence of the incoming beam. Kα fluorescence was used to determine the relative concentrations.

Results

Detailed measurements were made of the constituents of stainless steel and in particular Mo. Fig. 2a shows x-ray intensities for a scan across the salt layer at the steel/solution interface at a pit depth of 2 mm, and a controlled potential of 3.0 Vsce. In this scan each measurement was for 10s, at increments of 2 μm. Fig 3a shows similar measurements of Fe intensities for a series of potentials from 0.8 to 3.8 Vsce. Here the pit depth was about 2.5 mm, the step size was 1μm and counting was for 10 s. Fig. 4a show results from two scans across the solution within the pit at 20 μm steps between points. Only Fe results are shown for the earlier scan at 1.2 Vsce with a counting time of 15s per point. . The later scan after 4.7 h shows Fe, Cr, Ni and Mo, at 1.6 Vsce with a counting time of 10s.

Discussion

In Fig. 2a the highest intensities for Fe, Cr, Ni, and Mo were over the steel and decreased dramatically as the beam passed from metal to solution and the area density (i. e. the mass per unit area penetrated by the beam) of steel constituents dropped by a factor of about 28. The observed drops were less than 7.5 Comparison of the intensities is complex. The relative x-ray intensities of the elements depend on many factors, including the atomic number and the concentration of each element and thickness of the sample. For thick samples the fluorescence produced far below the surface is absorbed within the sample. The fluorescence energy is also important. For example, the Ni intensity over the steel, was higher than that of Cr even though it had a lower concentration, and Mo with one fourteenth of the atomic concentration gave an x-ray intensity of one half that of Cr. This arises because the lower energy of the Cr fluorescence is absorbed to a greater degree than the higher energy of the Ni and Mo fluorescence. Decreased area density of

alloy constituents in the solution, however, favors the intensities from the heavier elements. This arises because there is less absorption of the fluorescence from the heavier elements by the lighter elements. Thus, the Mo signal from the solution was greater than that of the Cr. The relative change in the intensities is clearer from the ratios of the intensities across the interface as shown in Fig. 2b. In every case the ratio of a heavier over a lighter element is larger when the beam is over the solution. This behavior is definitely not seen in the interfacial region in Fig. 2b where the salt layer is present. Here distnct peaks are observed because of major differences in concentrations of the elements in the salt layer associated with their transported across it. It has previously been shown for Type 304 stainless steel that the salt layer was high in Fe with smaller amounts of Ni and only very small concentrations of Cr remained in the salt (8).

Behavior of Mo in salt layers on stainless steel.

Salt layers precipitate on dissolving metal surfaces following supersaturation of the solution by the dissolution products. The salt layer and the concentrated solution within the pit are in a dynamic steady state as the cation flux within both must maintain the same stoichiometry and rate of dissolution of the alloy. In Fig 2b the presence of a salt layer and the cation composition relative to the metal is deducible from the peaks (8). The same sequence was expected for the Mo containing steels. Mo, being in the same group as Cr may behave similar to Cr. The results in Fig. 2b show that this was the case and very small fractions were present in the salt layer, but that the relative fraction was greater than that of Cr. Hence, Mo does not lead to any significant change in salt layers and the major changes in the corrosion resistance of the steels containing Mo could not be attributed changes in salt layer characteristics.

Previous studies up to 1 Vsce showed that the salt layer thickness increased with potential. The higher potentials were above those at which chromate could be expected. Chromates may be considered to replace chlorides in the salt layer and increase the ratio of Cr in the salt layer. Therefore thicker oxide layers were studied at higher potentials. In Fig 3a three consecutive Fe x-ray intensity measurements across the interface between 0.8 to 3.8 Vsce are shown. The corresponding Fe/Cr ratios in Fig. 3b showed peaks that increased with potential. The beam size was too large to give a direct measure of the salt layer composition necessitating modeling of changes in intensity with beam position. The modeling took into account the size of the x-ray beam as it scanned over the interface. This analysis led to the conclusion that a salt layer with a very low Cr concentration having a increasing thickness with potential, offered a satisfactory fit to the results. The models produced changes similar to the results in Fig. 3 leading to the conclusion that there were no significant changes in Cr or in chromate concentration at the higher potentials. The results were consistent with previous approaches where the salt layer thickness and resistance increased with potential to maintain a constant field in the salt layer to produce a constant diffusion controlled current.(8)

Behavior of Mo in concentrated localized corrosion solutions.

Fig 4 shows the intensities of Fe, Cr, Ni, and Mo in solution from close to the steel to the mouth of the pit. The two Fe curves taken at different times clearly show the same apparent scatter with distance, indicating excellent reproducibility. The non-linear variations were mainly due to the roughens of the sample produced during its manufacture and resulted in a marked variation the cross section. The Ni and to some

degree the Cr, also reflect the same behavior. The Cr a lower intensity and in this case is subject to a greater degree of scatter due to the intrinsic nature of the measurements. The slopes of the Fe, Cr and Ni curves were consistent with diffusion of soluble species, but because of the thickness variations, quantification of diffusion parameters was not attempted. Close to the metal the Mo displayed a similar behavior to the other elements, indicating it too was soluble and migrated away from the metal. However, with distance from the metal the Mo species showed an increase due to precipitation of an insoluble product. From a limited study using pit depths of 1 mm, no Mo precipitation was found. Hence, it is tentatively concluded that the precipitation of Mo is a slow process. The time of exposure of the pit walls to the pit solution decreases with distance from the pit mouth and the amount of Mo precipitated also decreases. A contribution due to a higher pH at the lower concentrations, cannot at present be excluded, but, because of the absence of a Mo build up for the smaller pit depth, it appears to be of lesser importance

Conclusions

1) A chloride salt layer rich in Fe formed on the surface of a Mo containing stainless steel during localized corrosion. The results suggest that Ni, Mo and Cr migrate more rapidly than Fe in the ferrous chloride layer.

2) Mo did not concentrate in the salt and initially formed a soluble product. Mo precipitation took place as the Mo species diffused from the dissolving interface probably as a result of slow kinetics rather than activity changes or pH increases nearer the mouth of the pit. Improved corrosion behavior of Mo containing stainless steels cannot be attributed to changes in the chemistry within pits or crevices.

3) Salt layers can be grown to high potentials above 3.8 Vsce, without observable changes in chromium content.

Acknowledgment

The x-ray fluorescent microprobe measurements were carried the Beamline X26A of the National Synchrotron Light Source at Brookhaven National Laboratory under Grants NASA NAG9 and NSF EAR86-18346. The work was performed under the auspices of the U.S. Department of Energy, Division of Materials Sciences, Office of Basic Energy Sciences under Contract No. DE-AC02-76CH00016.

References

1. S. Szklarska-Smialowska, *Pitting Corrosion of Metals,* Pub. National Association of Corrosion Engineers, Houston, 1986, p. 147.
2. M Uriquidi-Macdonald and D. D. Macdonald, in *Advances in Localized Corrosion,* H. Isaacs, U. Bertocci, J. Kruger and S. Smialowska Eds., National Association of Corrosion Engineers, Houston, 1990, p. 33.
3. R. C. Newman , *Corrosion Sci.,* **25**, 341 (1985).
4. J. R. Ambrose, *Corrosion* , **34** 27 (1979)
5. D A Stout J. B. Lumsden and R. W. Staehle, *Corrosion* , **35** 141 (1979)
6. Y. C. Lu, C. R. Clayton, A. R. Brooks, *Corrosion Sci.,* **29**, 863 (1989).
7. U. Steinsmo and H. S. Isaacs, *J. Electrochem. Soc.,* **140**, 643 (1993).
8. H. S. Isaacs, J.-H. Cho, M. L. Rivers, R. S. Sutton, *J. Electrochem. Soc.,* **142**, 1111 (1995).
9. H. S. Isaacs, J. *Electrochem. Soc.,* **120**, 1456 (1973).

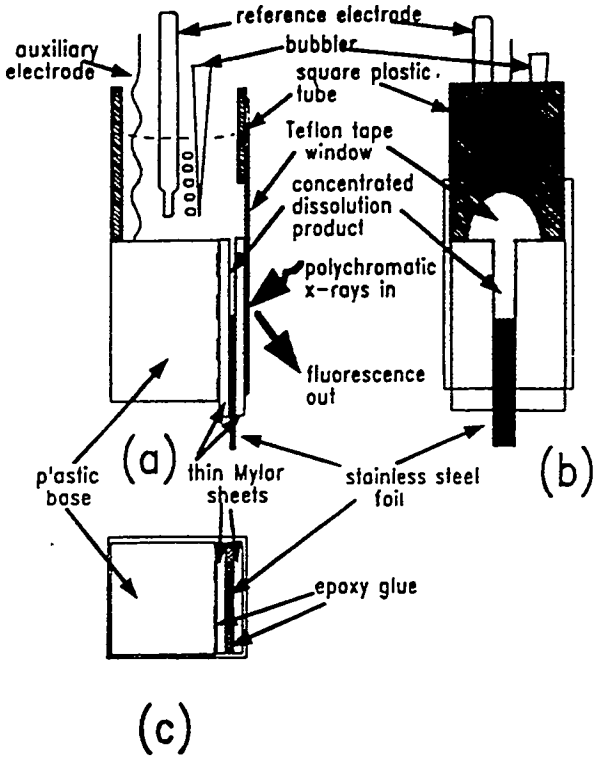

Figure 1. The cell with a simulated one-dimensional pit used for x-ray fluorescence microprobe measurements. (a) Vertical cross section of cell through the foil. (b) Horizontal cross section through the foil. (c) Front view of cell.

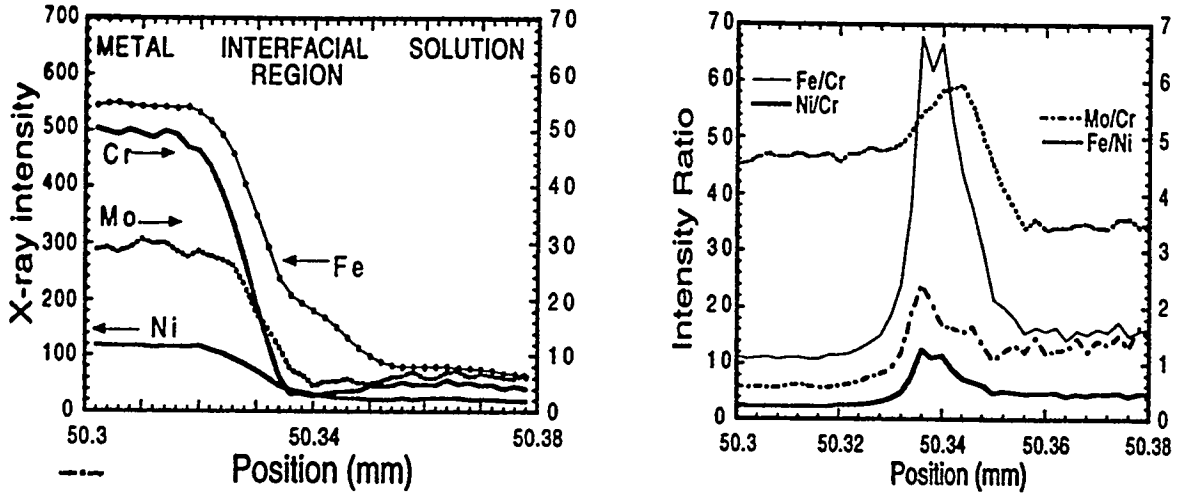

(a) (b)

Figure 2. (a) Variations of x-ray intensity for Fe Cr, Ni and Mo across the steel/solution interface at a potential of 3 Vsce, (b) Ratios of the x-ray intensities of elements shown in (a) across the interface

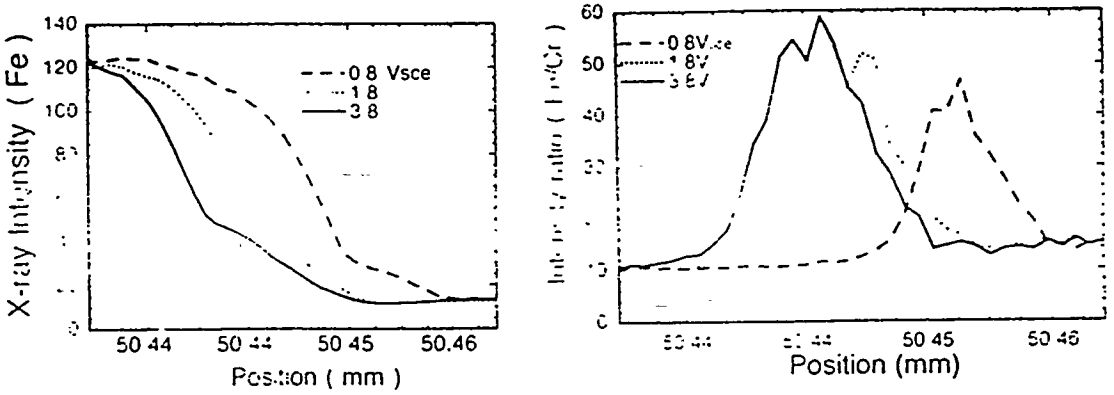

Figure 3. (a) Variations of x-ray intensity for Fe across the steel/solution interface at a potential of 0.8, 1.8 and 3.8 Vsce, (b) Fe/Cr x-ray intensity ratios for the scans in (a)

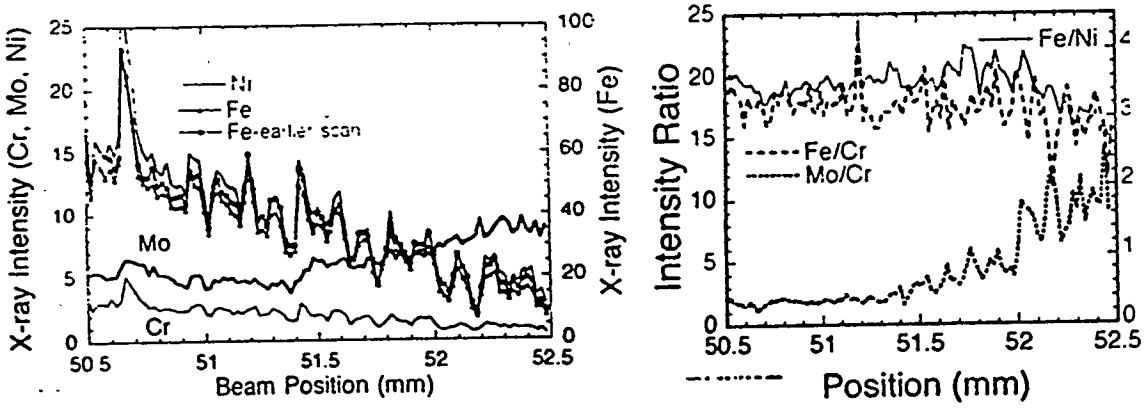

Figure 4. (a) Variation of intensity of dissolved elements in the artificial pit solution and a comparison with an earlier superimposed scan for Fe (Fe-2). (b) Variations in the intensity ratios of Fe/Cr, Fe/Ni and Mo/Cr across the solution.